Romanian Reports in Physics, Vol. 63, No. 1, P. 76–85, 2011

COLD FUSION FOR SUPERHEAVY ELEMENTS SYNTHESIS

P. STOICA[1,2]

[1]"Horia Hulubei" National Institute for Physics and Nuclear Engineering, P.O. Box MG 6, RO-077125, Bucharest-Magurele, Romania
[2]Canberra Packard SRL, Clejani 15, 051034 Bucharest, Romania, E-mail: paul.stoica@yahoo.co.uk

Received May 25, 2010

Abstract. The cold fusion phenomenon for the synthesis of $^{270}108$ superheavy nucleus within the macroscopic-microscopic method based on the two center shell model is investigated, in order to find the best projectile-target combination for its production. The fission/fusion yields are estimated by using the semiclassical WKB approach. Several asymmetric combinations of relative long living fragments, which can be used in fusion experiments of the superheavy nucleus with $A = 270$ and $Z = 108$ are evidenced.

Key words: superheavy nuclei, fusion reactions, macroscopic-microscopic model.

1. INTRODUCTION

Only 278 nuclides are found in the nature among about 3000 actually known. The synthesis of superheavy elements beyond $Z = 104$, suggested by Flerov [1], was predicted within the so-called fragmentation theory in Ref. [2] by using the cold valleys in the potential energy surface between different combinations, giving the same compound nucleus. Soon it was shown in Refs. [3, 4] that the most favorable combination with $Z > 104$ are connected with the so-called Pb potential valley, i.e. the same valley of the heavy cluster emission.

Due to the double magicity of ^{48}Ca, similar with ^{208}Pb, in Ref. [5] it was proposed ^{48}Ca as a projectile on various transuranium targets. Indeed, the production of many superheavy elements with $Z < 119$ (corresponding to the last stable element Cf) during last three decades was mainly based on this idea [6–8].
The formation of superheavy compound systems by fusion was intensively explored [9–11]. On the other side the investigation of experimental data concerning fusion and fission of superheavy nuclei with $Z = 112$, 114, 116, together with data on survival probability of these nuclei in evaporation channels with

3–4 neutrons, revealed the fact that the fission barriers are quite high, leading to a relative high stability of such systems [12].

The main tool to investigate such nuclei is almost exclusively based upon the investigation of α-decay chains. In the last decade several papers were devoted to the calculation of α-decay half-lives in this region. All these approaches can be considered as phenomenological ones, based essentially on the Gamow α-nucleus potential picture [13]. The recent microscopic estimate of the α-particle preformation factor, by using shell model single particle orbitals, performed in Ref. [14], showed that the strong change of the Q-value along neutron chains can by explained only by supposing the existence of an α-cluster component in heavy and superheavy emitters.

Recently, the production of $Z > 120$ superheavy elements was investigated using the macroscopic – microscopic model based on the two center Woods-Saxon shell model [15]. The same model will be used in the present paper to determine optimum beam target combination for the production of hassium. Using cold fusion reactions the elements bohrium ($Z = 107$), hassium ($Z = 108$) and meitnerium ($A = 109$) were synthesized from 1981 to 1984 [8]. The 108 element was obtained using the reaction ^{58}Fe+^{208}Pb [16].

2. THE MODEL

The microscopic-macroscopic model [17], as described in Ref. [18], is exploited dynamically. The dynamical analysis of a reaction requires at least the knowledge of the deformation energy V and the effective mass B. For simplicity, it is considered that these quantities depend upon the shape coordinates. So, in our analysis, the basic ingredient is the nuclear shape parametrization. Our nuclear shape parametrization is given by two ellipsoids of different sizes smoothly joined by a third surface obtained by the rotation of a circle around the axis of symmetry [19, 20]. Five degrees of freedom characterize this parametrization: the elongation given by the inter-nuclear distance $R = z_2 – z_1$ between the centers of the ellipsoids, the two deformations of the nascent fragments denoted by the eccentricities $\varepsilon_i=[1–(b_i/a_i)^2]^{1/2}$ (i=1, 2), the mass asymmetry obtained within the major semi-axis as $\eta=a_2/a_1$ and the necking parameter related to the curvature of the intermediate surface $C=s/R_3$. The meaning of the geometric symbols can be understood by inspecting the Fig. 1.

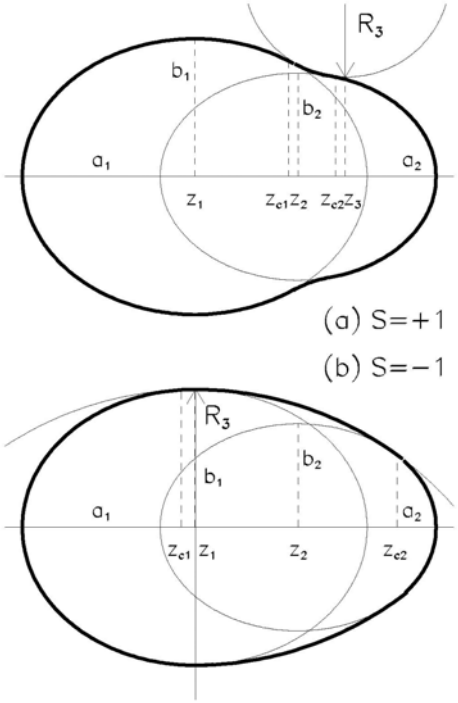

Fig. 1 – The nuclear shape parametrization.

The deformation energy was obtained by summing the liquid drop energy with the shell and the pairing corrections.

$$V = E_{LDM} + \delta E. \tag{1}$$

The macroscopic energy E_{LDM} is obtained in the framework of the Yukawa – plus – exponential model extended for binary systems with different charge densities [21] as detailed in Ref. [17]:

$$E_{LDM} = E_n + E_C + E_V, \tag{2}$$

where

$$E_n = -\frac{a_2}{8\pi^2 r_0^2 a^4} \iint_V \left(\frac{r_{12}}{a} - 2\right) \frac{\exp\left(-\frac{r_{12}}{a}\right)}{\frac{r_{12}}{a}} \mathrm{d}^3 r_1 \mathrm{d}^3 r_2 \tag{3}$$

is the nuclear term,

$$E_C = \frac{1}{2} \iint_\infty \frac{\rho_e(r_1)\rho_e(r_2)}{r_{12}} \mathrm{d}^3 r_1 \mathrm{d}^3 r_2 \tag{4}$$

is the Coulomb energy, and E_V is the volume energy. In the previous definitions ρ_e are charge densities and $r_{12}=|\mathbf{r}_1-\mathbf{r}_2|$. The numerical values of the parameters a_2, r_0, and a are taken from Ref. [22].

The shell effects δE are obtained as a sum between the shell δU and the pairing δP microscopic corrections. In this context, the Strutinsky procedure was used. These corrections represent the varying parts of the total binding energy caused by the shell structure. The single particle level diagrams are computed within the Woods-Saxon superasymmetric two-center shell model [23]. In calculating the pair corrections, the blocking effects are taken into account.

The effective mass is computed within the cranking adiabatic approximation [24-26]. In a multidimensional deformation space, where the nuclear shape is described by a set of n independent generalized coordinates $\{q_i\}$ (i=1,...,n), the inertia tensor B_{ij} is defined by the equation of the kinetic energy T:

$$T=\frac{1}{2}\sum_{i,j=1}^{n}B_{ij}(q_{1,}...q_n)\frac{\partial q_i}{\partial t}\frac{\partial q_j}{\partial t}. \tag{5}$$

In the adiabatic description of the collective behaviour of a nucleus, the nucleons are assumed to move in a average deformed potential. Using a Hamiltonian $H(q_1,\ldots q_n)$ that includes pairing interactions, introducing the collective parameters $\{q_i\}$ by means of the Lagrange multipliers, it is possible to obtain the response of the nuclear system for slow changes of the shape from the cranking model formula:

$$B_{ij}(q_{1,}...q_n)=2\hbar^2\sum_{\mu,\nu}\frac{\left\langle \mu\left|\frac{\partial H}{\partial q_i}\right|\nu\right\rangle\left\langle \nu\left|\frac{\partial H}{\partial q_j}\right|\mu\right\rangle}{(E_\mu+E_\nu)^3}(u_\mu v_\nu+u_\nu v_\mu)^2+P_{ij}, \tag{6}$$

where $|\nu>$ and $|\mu>$ are single particle wave functions, E_μ, u_μ and v_μ are the quasiparticle energy, the vacancy and occupation amplitudes of the state μ, respectively, in the BCS approximation, and P_{ij} is a correction that depends on the variation of the parameters Δ (the pairing gap) and λ (the Fermi energy) as function of the deformation coordinates. P_{ij} depends on the variations of the Fermi energy and of the pairing gap. Recently, the cranking model was improved by taking into account the intrinsic excitation produced during the fission process itself [25] by using time dependent equations of motion [27, 30]. The semi-adiabatic cranking model [25] predicts lower values of inertia than the adiabatic ones, similar to that given by the Gaussian overlap approximation [31]. The inertia B along a trajectory in the configuration space spanned by the generalized coordinates q_ν (ν= 1, 5) can be obtained within the formula

$$B=\sum_{\nu=1}^{5}\sum_{\mu=1}^{5}B_{\nu\mu}(q)\frac{\partial q_\nu}{\partial R}\frac{\partial q_\mu}{\partial R}, \tag{7}$$

where R is the generalized coordinate associated to the elongation.

The single particle states and wave functions needed for the calculation of the shell effects and the cranking inertia are obtained with a recent version of the superasymmetric two center shell model. This version solves a Woods-Saxon potential, consistent with the nuclear shape parametrization presented above, within the analytic semi-symmetric eigenvector basis of the two center harmonic potential [32]. The superasymmetric two center shell model was extensively used to investigate the fission process [33–39], the cluster [40–43] and alpha-decay [44, 45]. It must be mentioned that the alpha-decay is treated in an alternatively manner in this article, that is, using the microscopic-macroscopic approach in a wide range of mass asymmetries. This model is especially designed for fission processes. The conventional picture for alpha decay can be found in Refs. [46–49]. Other attempts to characterize single particle states within the mean field concept were realized in Ref. [50]. In this work, the major quantum number, that is the maximal number of radial nodes, used in our calculation is $N = 12$. To our knowledge, this formalism is the sole model able to calculate the microscopic part in the macroscopic-microscopic framework for the large asymmetries involved in alpha- and cluster-decay. The two center potential formalism can be applied for many physical purposes. For example, this model was used recently to characterize the reflection asymmetric mean field [51].

3. RESULTS AND DISCUSSIONS

Our first step is to estimate the deformation energy of all binary partitions for the synthesis of the element $^{270}108$. For all possible combinations $A_1+A_2=270$ and $Z_1+Z_2=108$, the driving potential was calculated at the scission configuration by using the ground state deformations [52]. For a given combination (A_1, A_2), the partition (Z_1, Z_2) with the lower value of the driving potential was selected. Now, it is considered that the two partners fuse to form the superheavy element. The inter-nuclear distance between the two nuclei is decreased up the formation of a sole superheavy nucleus. The mass asymmetry is varied linearly from that of the final partition up to a reflection symmetry ($\eta=1$) assumed for the compound nucleus, the system is considered constricted ($R_3=0$) and the total volume is preserved during the process. The two dimensional potential surface V versus the fragment mass of the light partner A_2 and the inter-fragment distance R is plotted in the upper panel of Fig. 2. In the lower panel of Fig. 2, the associated cranking mass parameter B is plotted.

Table 1

The half-lives of the elements that address the best theoretical binary partitions

A_1	$T_{1/2}$	A_2	$T_{1/2}$
^{214}At	558 ns	^{56}V	216 ms
^{213}At	125 ns	^{57}V	0.35 s
^{212}Po	45.1 s	^{58}Cr	7 s
^{211}At	7.214 h	^{59}V	75 ms
^{210}Bi	5.012 d	^{60}Mn	51 s
^{209}Po	102 y	^{61}Cr	0.27 s
^{208}Bi	3.68×10^5 y	^{62}Mn	92 ms
^{207}Bi	32.9 y	^{63}Mn	0.29 s
^{206}Bi	6.243 d	^{64}Mn	89 ms
^{205}Bi	15.31 d	^{65}Mn	92 ms
^{168}Ho	2.99 m	^{102}Nb	1.3 s
^{167}Er	stable	^{103}Zr	1.3 s
^{166}Ho	26.83 h	^{104}Nb	4.9 s
^{165}Yb	9.9 m	^{105}Sr	> 150 ns
^{164}Ho	29 m	^{106}Nb	1.02 s
^{163}Er	75 m	^{107}Zr	150 ms
^{162}Er	stable	^{108}Zr	80 ms
^{161}Er	3,21 h	^{109}Zr	>150 ns
^{160}Dy	stable	^{110}Mo	0.27 s
^{159}Dy	144.4 d	^{111}Mo	200 ms
^{158}Dy	stable	^{112}Mo	> 150 ns

It can be observed, that some combinations, characterized by a lower barrier, are more likely suited for the synthesis of the $Z = 108$ element. This is especially clear from Fig. 3, where we plotted the maximum value of the potential surface in Fig. 2 as a function of the fragment mass number A_2. The light elements corresponding to the best partitions are marked on the plot.

The first relevant minimum of the potential surface in the region $A_2 = 60$ corresponds to the already mentioned nucleus ^{58}Fe. Unfortunately, the best theoretical binary partitions are unstable, as can be seen from Table 1. A second region with good candidates for the formation of superheavy elements is for $A_2 = 107$. The half-lives of the partners involved in the best partitions are also listed in Table 1.

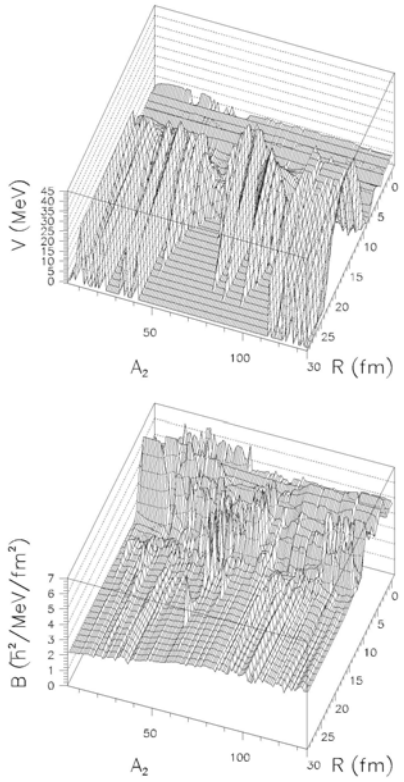

Fig. 2 – The two dimensional potential V and the cranking inertia B versus the light fragment mass number and the inter-fragment distance R, for the compound nucleus A=270 and Z=108.

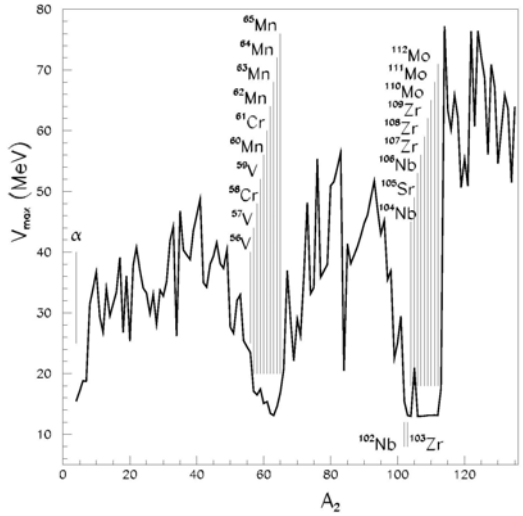

Fig. 3 – The maximum value of the potential surface in Fig. 2 with respect to the inter-fragment radius R, *versus* the light fragment mass number.

In order to search for reliable binary candidates, producing the above mentioned compound nucleus, it is necessary to investigate the penetration factor. This quantity can be estimated, as usually, by using the semiclassical integral

$$P(A_2) = \exp\left[-\frac{2}{\hbar^2}\int_{r_1}^{r_2}\sqrt{2V(R)B(R)}\mathrm{d}R\right] \tag{8}$$

between internal and external turning points. In Fig. 4 it is given the penetrability ratio $R=P(A_2)/P(\alpha)$, corresponding to the potential surface displayed in Fig. 2. Several maxima are present in this figure. They correspond to V, Cr, Mn, Nb, Sr, Zn, Mo projectiles. The most promising are the projectiles around Zr isotopes, where the half-lives are larger and where the greater penetrabilities are found.

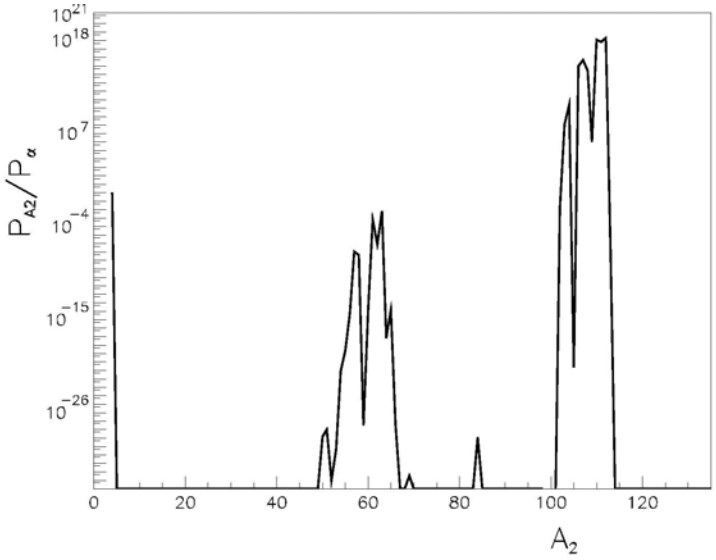

Fig. 4 – The normalized penetrabilities corresponding to the potential surface in Fig. 2 *versus* the mass number of the light fragment.

On the other hand the target-projectile combinations should be relative stable. In Table1 are given the fragment half-lives of these binary combinations, corresponding to local maxima of the penetrability. Unfortunately the half-lives of the heavy isotopes and their partners are very small. However, in the mass region indicated by our best two partitions ^{212}Po+^{58}Cr and ^{167}Er+^{103}Zr, they are several possibilities to find long lived elements, to be used in fusion experiments.

Concluding, the potential energy surface for different binary combinations, giving the superheavy compound nucleus ^{270}108 was computed in the frame of the macroscopic-microscopic method by using a recent version of the two center shell model based on the Woods-Saxon potential. The best suited binary partners for the

production of superheavy elements with $A = 270$ were evidenced. Two regions with good candidates for the formation of superheavy elements were identified.

Acknowledgments. This work is part of a Ph.D. Thesis realized under the supervision of prof. M. Apostol. The author is grateful to prof. D.S. Delion and to Dr. M. Mirea for fruitful discussions. This work was financed by the CNCSIS grants IDEI 512 and IDEI 119.

REFERENCES

1. G.N. Flerov, Atom. Ener., **26**, 138 (1969).
2. A. Sandulescu, R.K. Gupta, W. Scheid and W. Greiner, Phys. Lett., B **60**, 225 (1976).
3. R.K. Gupta, C. Parvulescu, A. Sandulescu and W. Greiner, Z. Phys., A **283**, 217 (1977).
4. R.K. Gupta, A. Sandulescu and W. Greiner, Phys. Lett., B **67**, 257 (1977).
5. Y.T. Oganessian, Nucl. Phys., A **685**, 17c (2001).
6. Y.T. Oganessian et.al, Nucl. Phys., A **734**, 109 (2004).
7. S. Hofmann and G. Munzemberg, Rev. Mod. Phys., **72**, 733 (2000).
8. S. Hofmann, G. Munzenberg and M. Schadel, Nucl. Phys. News, **14**, 5 (2004).
9. V.Y. Denisov and S. Hofmann, Phys. Rev., C **61**, 034606 (2000).
10. R. Smolanczuk, Phys. Rev., C **63**, 044607 (2001).
11. V.I. Zagrebaev, Y. Arimoto, M.G. Itkis and Y.T. Oganessian, Phys. Rev., C **65**, 014607 (2001).
12. M.G. Itkis, Y.T. Oganessian, V.I. Zagrebaev, Phys. Rev., C **65** 044602 (2002).
13. G. Gamow, Z. Phys., **51**, 204 (1928).
14. D.S. Delion, A. Sandulescu and W. Greiner, Phys. Rev., C **69**, 044318 (2004).
15. M. Mirea, D.S. Delion and A. Sandulescu, EPL, **85**, 12001 (2009).
16. G. Munzenberg, et al, Z. Phys., A **324**, 489 (1984)
17. M. Brack, J. Damgaard, A. Jensen, H. Pauli, V. Strutinsky and W. Wong, Rev. Mod. Phys. **44,** 320 (1972).
18. M. Mirea, O. Bajeat, F. Clapier, F. Ibrahim, A.C. Mueller, N. Pauwels and J. Proust, Eur. Phys. J., A **11**, 59 (2001).
19. M. Mirea, D.S. Delion and A. Sandulescu, Rom. J. Phys., **55**, 309 (2010).
20. I. Companis, M. Mirea and A. Isbasescu, Rom. J. Phys., **56**, *1–2*, 63–70 (2011).
21. D.N. Poenaru, M. Ivascu, and D. Mazilu, Comput. Phys. Commun., **19**, 205 (1980).
22. P. Moller and J.R. Nix, At. Data Nucl. Data Tables, **26**, 165 (1981).
23. M. Mirea, Phys. Rev., C **78,** 044618 (2008).
24. M. Mirea, R.C. Bobulescu and P. Marian, Rom. Rep. Phys., **61**, 646 (2009).
25. M. Mirea and R.C. Bobulescu, J. Phys., G **37**, 055106 (2010).
26. M. Petre, R.C. Bobulescu, C. Petre and M. Mirea, Rom. J. Phys., **55**, 741 (2010).
27. M. Mirea, Phys. Lett., B **680**, 316 (2009).
28. M. Mirea, Rom. J. Phys., **54,** 501 (2009).
29. M. Mirea, L. Tassan-Got, C. Stephan and C.O. Bacri, Nucl. Phys., A **735**, 21 (2004).
30. M. Mirea, Mod. Phys. Lett., A **18**, 1809 (2003).
31. A. Gozdz, K. Pomorski, M. Brack and E. Werner, Nucl. Phys., A **442**, 26 (1985).
32. M. Mirea, Phys. Rev., C **54**, 302 (1996).
33. M. Mirea, L. Tassan-Got, C. Stephan, C.O. Bacri, P. Stoica and R.C. Bobulescu, J. Phys., G **31**, 1165 (2005).
34. M. Mirea and P. Stoica, Rom. J. Phys., **50**, 517 (2005).
35. M. Mirea, L. Tassan-Got, C. Stephan, C.O. Bacri and R.C. Bobulescu, Europhys. Lett., **73**, 705 (2006).
36. M. Mirea, L. Tassan-Got, C. Stephan, C.O. Bacri and R.C. Bobulescu, Phys. Rev., C **76**, 064608 (2007).
37. M. Mirea and L. Tassan-Got, Cent. Europ. J. Phys., **56**, *9–10*, 116 (2011).
38. M. Mirea and L. Tassan-Got, Rom. J. Phys., **54**, 331 (2009).

39. M. Mirea, D.S. Delion and A. Sandulescu, Phys. Rev., C **81**, 044317 (2010).
40. M. Mirea, Nucl Phys., A **780**, 13 (2006).
41. M. Mirea, Europ. Phys., J. A **4**, 335 (1999).
42. M. Mirea, Phys. Rev., C **57**, 2484 (1998).
43. M. Mirea and F. Clapier, Europhys. Lett., **40**, 509 (1997).
44. P. Stoica, in Proceedings of International Workshop on *New Applications of Nuclear Fission*, Sept. 07-12 2003, Bucharest, World Scientific, Singapore, p. 174, 2004.
45. M. Mirea, Phys. Rev., C **63**, 034603 (2001).
46. I. Silisteanu, M. Rizea, B.I. Ciobanu and A. Neacsu, Rom. J. Phys., **53**, 1191 (2008)
47. I. Silisteanu, A.I. Budaca and A.O. Silisteanu, Rom. J. Phys., **55**, 1088 (2010).
48. I. Silisteanu, A. Neacsu, A.O. Silisteanu and M. Rizea, in Proceedings of the Carpathian Summer School in *Physics Exotic Nuclei/Particle Astrophysics (II)*, 20-31 August 2007, AIP Conference Proceedings 972, p. 505, 2008.
49. D.S. Delion and M. Boscoianu, Rom. J. Phys., **54**, 587 (2009).
50. R.A. Ionescu and C. Hategan, Rom. Rep. Phys., **62**, 18 (2010).
51. P. Jiao, J.-Y. Gun and X.-Z. Fang, Acta Physica Sinica, **59**, 2369 (2010).
52. P. Moller, J.R. Nix, W.D. Myers and W.J. Swiatecki, At. Data Nucl. Data Tables, **59**, 185 (1995).